CrossMark

RESEARCH ARTICLE

Smectites and zeolites in ash from the 2010 summit eruption of Eyjafjallajökull volcano, Iceland

M. Paque [1] · M. Detienne [1] · E.C. Maters [1] · P. Delmelle [1]

Abstract Hydrothermal alteration minerals are often incorporated in volcanic ash from phreatic and phreatomagmatic activity. Here we assess the presence and abundance of such minerals in the ash materials produced during the April-May 2010 initial phreatomagmatic (*phase I*) and subsequent magmatic (*phases II* and *III*) eruptions of Eyjafjallajökull volcano, Iceland. The results of X-ray diffraction analyses reveal significant quantities of smectites (up to 4 wt%, mainly as saponite) and zeolites (up to 7 wt%) in ash from *phase I*. While a minor amount of smectites (<0.5 wt%) is present in ash from the subsequent weak explosive activity (*phase II*), both smectites and zeolites are absent in *phase III* ash. This material was generated following abrupt rejuvenation of explosive activity in the absence of magma-ice/water interaction. Smectites and zeolites in *phase I* ash result primarily from scouring of altered volcanic rocks in the subsurface, although some may derive also from water-rock interaction within the summit ice cauldrons through which fragmented magma was injected. We show that incorporation of smectites and zeolites in *phase I* ash can explain its anomalously high specific surface area. Further, the presence of these minerals in ash may enhance its ability to act as ice nuclei as well as favour particle aggregation processes in the volcanic plume/cloud. Finally, the Eyjafjallajökull eruption represents another case in which ash fallout acted as an exogenic source of 2:1-type clay minerals in volcanic soils.

Keywords Eyjafjallajökull volcano · Ash · Smectites · Zeolites · Hydrothermal alteration · Palagonitisation

Editorial responsibility: P. Allard

✉ P. Delmelle
  pierre.delmelle@uclouvain.be

[1] Environmental Sciences, Earth and Life Institute, Université catholique de Louvain, Croix du sud 2, bte L7.05.10, 1348 Louvain-la-Neuve, Belgium

Introduction

Subsurface aqueous environments are a common feature of ice-capped volcanoes (e.g. Björnsson 2003; Favier et al. 2008; Garchar et al. 2012). When a temperature gradient develops in response to magma intrusion at shallow depth within a glacier-covered volcano, melting at the base of the ice cap may act as a source of water for the establishment of hydrothermal convection cells. The ubiquitous occurrence of deposits such as hyaloclastites and hyalotuffs on volcanoes beneath glaciers (Loughlin 2002 and references therein) also attests to liquid water in these environments. Water within active volcanoes is usually synonymous with enhanced rock alteration. For glacier-covered edifices, evidence of pervasive rock alteration comes from geological studies of subglacial volcanic deposits (e.g. Loughlin 1995, 2002) and mineralogical analyses of Icelandic jökulhlaup materials (e.g. Cousins et al. 2013; Warner and Farmer 2010).

Eyjafjallajökull volcano in south Iceland erupted in 2010 and caused severe problems for air traffic due to dispersion of the ash clouds over Europe (Gudmundsson et al. 2012). The volcano is covered by a glacier and was formed over the last 0.78 Ma by numerous eruptions involving varying degrees of magma-ice interaction (Kristjansson et al. 1988; Loughlin 2002). The 2010 explosive activity of Eyjafjallajökull punched through the summit ice cap, and based on the above considerations, there is good reason for conjecture that it

disrupted subsurface altered rocks. Here we test this hypothesis by assessing the presence and quantifying the abundances of alteration minerals in ash fallouts from the eruption. We then discuss the potential implications of our findings.

Materials and methods

Eyjafjallajökull is a central volcano of Iceland's eastern volcanic zone, which runs southwest from Vatnajökull to Vestmannaeyjar off the south coast (Fig. 1). It rises from sea level to an elevation of about 1660 m and covers an area of about 400 km^2. The volcano is capped by an 80 km^2 glacier above 1000 m elevation; the thickness of the ice varies between 200 and 400 m in the summit caldera to less than 100 m on the edifice slopes (Magnússon et al. 2012). Eyjafjallajökull has previously erupted mainly transitional alkali basalts with minor ankaramite to quartz trachyte compositions (Loughlin 1995 and references therein). The ubiquitous occurrence of proximal lithofacies associations such as lava sheets, massive hyaloclastites and hyalotuff points to subglacial eruptions (Loughlin 2002).

The 39-day-long summit eruption of Eyjafjallajökull took place in April-May 2010 after 187 years of repose and was a moderate size event (VEI = 3). Four distinct eruptive phases, and corresponding ash fallout distributions, are described by Gudmundsson et al. (2012): *phase I* (14–18 April) was characterised by intense magma-ice interaction resulting in extensive ice melting and alternating emission of steam-rich and ash-rich plumes. During this explosive phase, ash affected a sector towards the east (14–16 April) and to the south (17 April). *Phase II* (18 April–4 May) featured comparatively limited magma-ice/water interaction and weaker explosive activity which led to local ash falls. *Phase III* (5–17 May) was marked by abrupt rejuvenation of explosive activity and an absence of magma-ice/water interaction, resulting in considerably wider ash dispersal than in the first explosive phase. *Phase IV* (18–22 May) corresponded to the progressive decline in explosive activity and termination of the eruption. About 140×10^6 m^3 of ash fell in Iceland, i.e. roughly 50 % of the total amount of airborne ash produced by the eruptions. Magma composition was benmoreitic during *phase I* but renewed explosivity in *phase III* was driven by a trachytic melt (Sigmarsson et al. 2011).

We studied eight ash samples from the 2010 eruption of Eyjafjallajökull (four from *phase I*, two from *phase II* and two from *phase III*); a brief sample description is provided in Table 1. The ash materials were collected at various distances within approximately 38 km downwind of the volcano summit (Fig. 1). Where possible, the ash from *phase I* was sampled from clean and dry surfaces (bench, window sill, plastic chair, etc.). The ash materials from *phase II* and *phase III* were collected using clean plastic containers during or immediately

after the eruptions. All samples correspond to ash which upon deposition has neither been affected by water or snow nor been in contact with the soil surface. The bulk ash compositions are given in the Supplementary material (Table S1) and conform with previous analyses (e.g. Gislason et al. 2011; Sigmarsson et al. 2011).

The ash mineralogy was determined by X-ray diffraction (XRD) using a Bruker D8 Advance instrument operated at 40 kV and 30 mA, with a step width of 0.02° and a counting time of 2.0 s $step^{-1}$, using Kα radiation sourced from a Cu target anode. All samples were ground to fine powders in an agate mortar prior to analysis. Crystalline minerals were identified using the EVA© software and the PDF-2 (International Centre for Diffraction Data 2013) and EVA©-embedded DiffracPlus Reference databases. The proportions of different crystalline minerals in the ash were calculated using the Siroquant© 4.0 software, which includes a comprehensive clay library containing over 48 clay minerals (Taylor and Matulis 1991). Based on Rietveld principles (Rietveld 1969; Bish and Post 1993), Siroquant© uses full profile fitting routines to generate a synthetic pattern that can be systematically refined via a least-squares minimisation of the difference with the diffraction pattern obtained experimentally. In order to be able to quantify the proportions of each crystalline mineral in ash, the amorphous glass content must be known. The latter is estimated by spiking the sample with an internal standard (here we used 10 wt% of Si) followed by re-analysis under the same XRD operating conditions as described above. Further details on the use of an internal standard to quantify the glass content in a polycrystalline sample are given by Winburn et al. (2000) and Ward and French (2006). The accuracy in the weight percent determination is limited by the crystal structure information available in the mineral databases and depends on the quality of the fit obtained. The protocol for mineral quantitative analysis used here produced an accuracy in the range of 5–10 % based on trials with synthetic mixtures comprised of two or three crystalline minerals (i.e. quartz, kaolinite and silicon) and volcanic glass (rhyolite) in known amounts.

Additional XRD measurements were conducted on the clay-sized fraction (<2 μm) of sample EYJ-A3 to determine more precisely the composition of clay minerals in the *phase I* ash. The <2-μm size separate was obtained by shaking the sieved fraction <50 μm of the ash material with a Na-resin to ensure clay dispersion followed by time settling in deionised water (Pansu and Gautheyrou 2006). The resin promotes cation exchange between Na^+ and flocculating cations at the clay surface, thereby acting to stabilise the clay suspensions. The <2 μm size separate was subject to various chemical pre-treatments: an aliquot was saturated with K and heated to 105, 300 and 500 °C, whereas another aliquot was saturated with Mg and then solvated with ethylene glycol (Pansu and Gautheyrou 2006 and references therein). The positions,
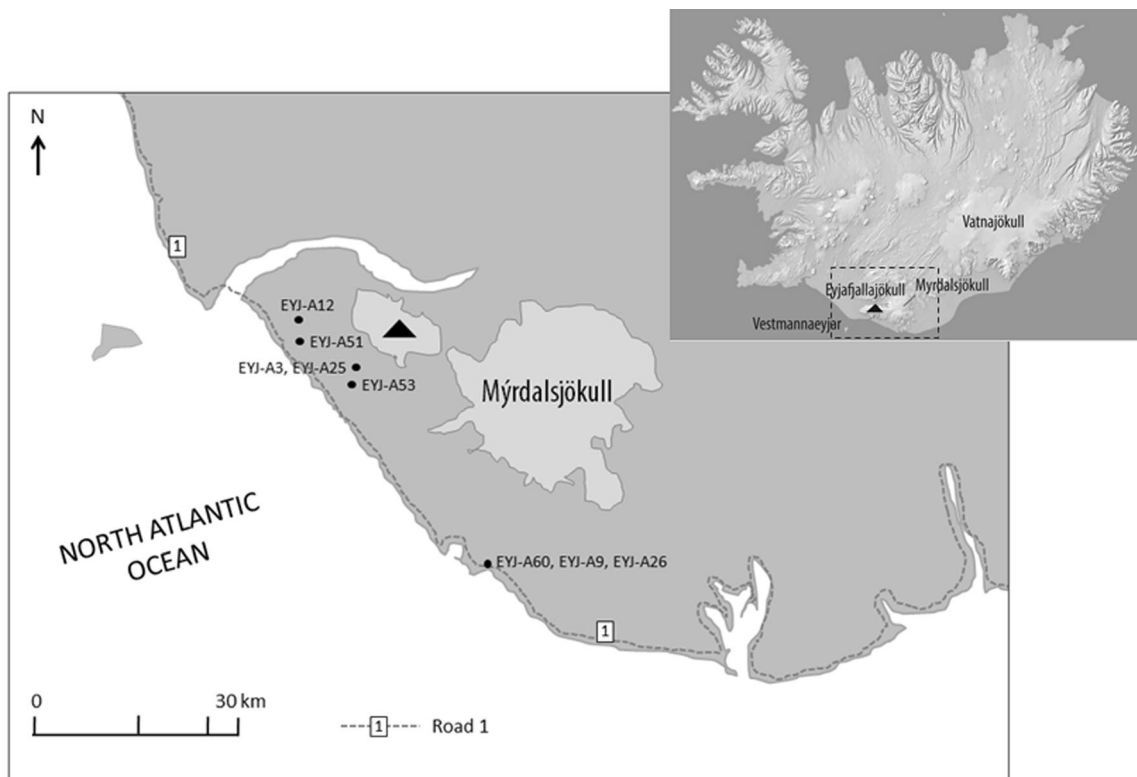
Fig. 1 Simplified maps showing Eyjafjallajökull volcano (*black triangle*) in Iceland and ash sample collection locations (*black circles*) downwind of the volcano. The Myrdalsjökull and Vatnajökull glaciers are also represented. See text and Table 1 for further description of the ash samples

shapes and intensities of the XRD peaks, and the changes in these parameters between sample treatments, enable the identification of different clay minerals. The effect of preferred orientation of mineral grains on reflection peak intensities during XRD analysis was minimised by using randomly oriented powder mounts (Fejdi and Holocsy 2001).

Results

The mineral assemblages identified in the *phase I, phase II* and *phase III* ash samples are given in Table 2 and representative XRD diffractograms (EYJ-A3, EYJ-A12 and EYJ-A25) are shown in Fig. 2 (the entire dataset is

Table 1 Brief description of the ash samples used in this study

	Eruption date	Sampling date	Site coordinates Northing/easting (UTM)	Distance from the volcano (km)
Phase I				
EYJ-A60	14 April 2010	14 April 2010	7033801/599214	37.7
EYJ-A3[a]	14-17 April 2010	22 April 2010	7048606/568456	8.5
EYJ-A51	17 April 2010	17 April 2010	7047552/559907	13.2
EYJ-A53	17 April 2010	18 April 2010	7046144/430505	10.75
Phase II				
EYJ-A9	23 April 2010	23 April 2010	7067632/543960	37.7
EYJ-A12	24 April 2010	24 April 2010	7050205/557993	13.3
Phase III				
EYJ-A26	7 May 2010	7 May 2010	7033717/600257	37.7
EYJ-A25	9 May 2010	9 May 2010	7048421/568454	7.9

[a] Composite sample shielded from rain

provided as Supplementary material, Fig. S1). The higher background noise observed in the 15–40 2θ region of all XRD diffractograms is due to amorphous glass within the ash. All ash samples contain the major primary magmatic minerals including plagioclases, pyroxenes and titanomagnetite. However, the *phase I* ash clearly displays additional XRD peaks between 5 and 6 2θ which are not present in the *phase II* and *phase III* specimens. These peaks typically correspond to clay minerals. Zeolite minerals are also identified in the *phase I* ash but not in the other samples.

Further XRD analyses of the <2-μm fraction of EYJ-A3 ash subjected to chemical and thermal treatment reveal a pattern typical of smectites; the d(001) peak is at 6 2θ (~14 Å) in the untreated sample but shifts to 5.2 2θ (~17 Å) with exposure to ethylene-glycol and breaks down to 9.5 2θ (~10 Å) upon heating to 500 °C (Fig. 3). A well-defined peak at 60.2 2θ (~1.54 Å; Fig. 4) identifies saponite, i.e. a trioctahedral Fe/Mg smectite, as the major clay mineral in the <2-μm fraction, although minor montmorillonite (a dioctahedral smectite) may also be present. Zeolites (possibly dominated by analcime) are also found in this size fraction.

Results of the quantitative mineralogical analysis are compiled in Table 2. Crystalline minerals in all the ash samples are dominated by plagioclases (~25–38 wt%) followed by pyroxenes (~5–15 wt%). The glass content varies between 50 and 59 wt%. Smectites and zeolites in the *phase I* ash occur in significant amounts, i.e. ~4 and ~3–7 wt%, respectively. Based on the analysis of the EYJ-A3 sample, smectites are the dominant crystalline mineral (~17 wt%) in the <2-μm fraction of the *phase I* ash. However, the clay-sized fraction accounts for only 3 wt% of the bulk ash, and therefore, most of the zeolite and smectite materials are associated with coarser ash grains.

While XRD peaks indicative of clay and zeolite minerals are not visible in the diffractograms of the *phase II* and *phase III* ash, EYJ-A12 displays a slight background elevation in the region 3–6 2θ. Although strongly attenuated, this feature seems to have shifted towards lower 2θ values upon Mg saturation (Supplementary material, Fig. S2), possibly revealing the presence of smectites but in very low amounts. Spiking of EYJ-A12 with 0.5 wt% of pure smectite (montmorillonite) suggests that the content of smectites, if present, in the *phase II* is <0.5 wt% (Supplementary material, Fig. S3).

Discussion

Origin of smectite and zeolites in *phase I* ash

Our mineralogical analyses indicate that smectites (mainly saponite) and zeolites occur in the *phase I* ash in non-negligible quantities. These minerals are commonly encountered in active hydrothermal systems where alteration of basaltic rocks takes place under neutral to mildly alkaline conditions and at temperatures generally below 200 °C (e.g. Browne 1978; Utada 2001). Smectites and zeolites also typically form during palagonitisation, i.e. the complex dissolution-precipitation reactions responsible for alteration of glassy basaltic lava and ash in low-temperature (<120 °C), water-rich environments (Stroncik and Schmincke 2002). Palagonitisation is generally thought to be both time- and temperature-dependent.

There is a strong indication that the subsurface rocks at Eyjafjallajökull volcano are altered to various degrees. Loughlin (1995) indicates that the subglacial hyaloclastite breccias and lavas near the core of the volcano are hydrothermalised, although the alteration mineralogy is not known. While we are not aware that Eyjafjallajökull hosted an active hydrothermal system prior to the 2010 eruption, recurrent sill episodes in the volcano (Loughlin 1995) probably enabled the development of temporary shallow hydrothermal convection cells. In addition, Loughlin (1995, 2002) also reports pervasive palagonitisation of hyaloclastite and hyalotuff deposits, likely the result of water-rock interaction during subglacial emplacement of volcanic eruption products.

Smectites in fresh ash deposits has been reported at other volcanoes, including Mt. Shinmoe-dake, Kirishima (Kanno et al. 1961), Usu (Kondo et al. 1978) and Akita-Akeyama (Nogami et al. 2000) in Japan; Soufrière in Guadeloupe (Cadiboche et al. 1987); and Mt. St. Helens in the USA (Pevear et al. 1982). In contrast to smectites, there is seldom evidence of zeolites in ash (Ohba and Nakagawa 2002). The source of smectites (and other alteration minerals) in ash has been invariably linked to fragmentation of altered rocks in the volcanic conduit, most often during phreatic or phreatomagmatic activity (e.g. Pevear et al. 1982; Mizota and Faure 1998; Ohba and Kitade 2005). Similarly, fragmentation of subsurface altered rocks (i.e. hydrothermalised and palagonitised hyaloclastite and hyalotuff deposits) present in the volcanic conduit may account for incorporation of smectites and zeolites in the Eyjafjallajökull ash produced during *phase I* of the eruption. Examination by optical microscopy of sand-sized (>50 μm) particles separated from EYJ-A3 ash (*phase I*) lends credence to this hypothesis as it reveals fresh glassy fragments mixed with fewer altered ones. As the eruption progressed, scouring of the conduit wall rocks became a minor process and smectites and zeolites were no longer incorporated in the ash mixture. In agreement with Dellino et al. (2012), this may simply reflect that the volcanic conduit was already well established at the end of the initial phreatomagmatic eruptive phase.

An additional mechanism may be evoked to explain the presence of smectite and zeolite minerals in the ash fallout from *phase I*. As proposed earlier, this eruptive stage was characterised by injection of an already fragmented magma

Table 2 Mineralogy of the ash samples as determined by X-ray diffraction and using Siroquant© software. The mineral contents are reported in weight percent

	Phase I			Phase II			Phase III		
	EYJ-A60	EYJ-A3	EYJ-A3[a]	EYJ-A51	EYJ-A53	EYJ-A9	EYJ-A12	EYJ-A26	EYJ-A25
Plagioclases	29.6	30.3	13.6	38.3	25.5	33.2	31.8	31.3	37.5
Pyroxenes	6.6	4.6	4.0	5.0	5.5	6.6	8.4	15.0	6.5
Fe.Ti oxides	1.2	1.9	2.4	2.6	1.9	6.6	2.5	3.4	2.2
Smectites[b]	4.4	4.4	17.2	4.5	4.1	n.d.	n.d.[c]	n.d.	n.d.
Zeolites	7.0	5.6	4.9	3.0	3.9	n.d.	n.d.	n.d.	n.d.
Glass	51.2	53.0	57.7	46.5	58.9	53.1	57.2	50.3	53.8

n.d. not detected

[a] Size fraction <2 μm

[b] Mostly as saponite but minor montmorillonite may also be present

[c] Spiking of this ash with pure montmorillonite suggests that smectites, if present, are <0.5 wt%

through ice cauldrons formed over the summit vent (Gudmundsson et al. 2012; Magnússon et al. 2012). According to Magnússon et al. (2012), ~0.08 km³ of the volcano ice cap was melted during the formation of ice cauldrons. These authors also indicate that ash and meltwater accumulated in the cauldrons before being flushed out in the evening of 15 April 2010. Cioni et al. (2014) further argued that a substantial proportion of the fragmented material erupted fell back into the ice/water filled vent before being expelled again by explosive eruption. Recycling of ash within the ice/water filled vent may have considerably increased the contact time between magma fragments and hot/boiling water, possibly allowing early palagonitisation reactions of glassy ash particles (Stroncik and Schmincke 2002). The smaller particles (i.e. with a higher surface area) would have been more reactive and susceptible to undergo such reactions. The altered material was then eventually entrained in the ash emissions leaving the vent. Such a scenario of in-vent ash alteration would be hindered in the later eruptive phases due to the formation of a tephra cone inside the ice cauldron which effectively isolated the rising fragmented magma from the surrounding glacier (Cioni et al. 2014).

Potential influence of smectites and zeolites on the properties of *phase I* ash

According to Horwell and Baxter (2006), the proportion and composition of respirable-sized (<4 μm) material in ash is a critical parameter for assessing the health hazard posed by ash emissions. Previous analyses suggest that the respirable component in the *phase I* and *phase III* ash amounts to ~2–12 and ~2–5 vol%, respectively. Based on our XRD measurements, the respirable fraction in the *phase I* ash is comprised of smectites (dominated by saponite) and zeolites along with aluminosilicate glass and primary crystalline minerals. There is no data on the potential health effect resulting from chronic

inhalation of smectites, but the rare occupational studies suggest only mild non-specific tissue changes (World Health Organization 2005). The XRD diffractogram suggests analcime as the main zeolite in the *phase I* ash but other zeolite minerals may also exist. While non-fibrous zeolites such as analcime do not pose a health hazard, there is epidemiological evidence that exposure to fibrous zeolites (notably erionite) increases the risk for developing malignant mesothelioma in humans (IARC 2012). Since fibrous zeolites have been found in altered volcanic tuff elsewhere (e.g. Rom et al. 1983; Baris and Grandjean 2006), further mineralogical investigations are recommended to assess the precise zeolite mineral assemblage present in *phase I* ash.

Previous studies (Gislason et al. 2011; Horwell et al. 2013) report the specific surface area measured by gas adsorption and the Brunauer-Emmett-Teller (BET) method (SSA_{BET}) of ash specimens from *phase I* and *phase III*. The ash erupted during *phase I* systematically displays a markedly higher SSA_{BET} (up to 7.7 m² g⁻¹) compared to that exhibited by the ash emitted later (SSA_{BET} ~0.3–0.45 m² g⁻¹). We measured (Supplementary material, Table S2) the SSA_{BET} of EYJ-A3 (*phase I*) and EYJ-A26 (*phase III*) and our results (~5.7 and ~0.2 m² g⁻¹, respectively) confirm earlier findings. Gislason et al. (2011) claimed that the high SSA_{BET} of *phase I* ash was probably due to an elevated content of very fine particles, the underlying assumption being that the specific surface area of a powdered material is primarily dictated by the size of the particles of which it is composed. We computed the geometric specific surface area (SSA_{geo}) of the EYJ-A3 (*phase I*) and EYJ-A26 (*phase III*) specimens on the basis of their particle size distribution (Supplementary material; Fig. S4). The conventional assumption of this approach is that all particles are spherical. There is a large discrepancy between SSA_{geo} (~0.2 m² g⁻¹) and SSA_{BET} (~5.7 m² g⁻¹) for EYJ-A3. In contrast, similar values of SSA_{BET} and SSA_{geo} are found for EYJ-A26 (~0.2 m² g⁻¹). This result suggests that
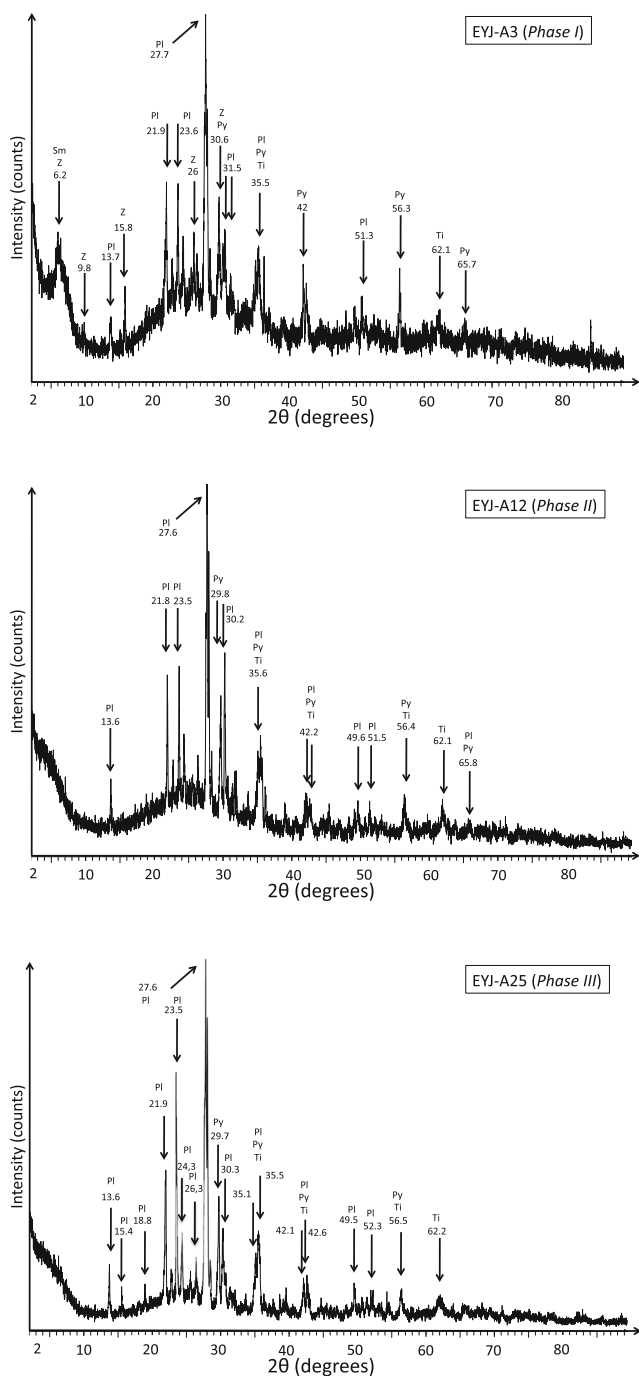
Fig. 2 X-ray diffractograms of ash samples EYJ-A3 (*phase I*), EYJ-A12 (*phase II*) and EYJ-A25 (*phase III*). The *arrows* indicate the main peaks corresponding to plagioclase (*Pl*), pyroxenes (*Py*), smectites (*Sm*), titanomagnetite (*Ti*) and zeolites (*Z*)

particle size distribution alone cannot explain the high SSA_{BET} values found for *phase I* ash.

Measured SSA_{BET} values of natural powdered materials commonly deviate from SSA_{geo} values. This is usually attributed to the spherical particle assumption which does not account for more complex particle morphology, and to surface features such as microporosity (pore diameter < 20 Å) and roughness (e.g. Brantley and Mellott 2000). While particle morphology and surface roughness may contribute to raise SSA_{BET} relative to SSA_{geo} of volcanic ash (Riley et al. 2003), there is no evidence that these changed dramatically over the course of the Eyjafjallajökull eruption (Dellino et al. 2012; Cioni et al. 2014). Microporosity can also be dismissed because micropores have been shown to represent a negligible contribution to ash porosity (Delmelle et al. 2005). Thus, the origin of the outstanding SSA_{BET} value of the *phase I* ash must be sought elsewhere.

We argue that the presence of smectites and zeolites in the *phase I* ash is responsible for both its high SSA_{BET} and the large discrepancy between SSA_{BET} and SSA_{geo}. Due to their meso- and microporous structure, smectites and zeolite minerals are well-known for developing remarkable SSA values, on the order of several 10s to 100s m^2 g^{-1} (e.g. Mertens et al. 2009; Kodama 2012). Assuming a conservative value of 100 m^2 g^{-1} for smectite and zeolites, it can readily be shown that a few weight percentages of these minerals in the *phase I* ash are sufficient to increase its SSA_{geo} by a factor of >10. This strongly suggests that smectites and zeolites in the *phase I* ash are responsible for the high SSA_{BET} values.

Since the SSA_{BET} of the *phase I* ash is significantly inflated by smectites and zeolites, caution is advocated when interpreting SSA_{BET}-normalised concentrations and release rates of soluble elements in ash leachate studies (e.g. Gislason et al. 2011; Horwell et al. 2013). In particular, this applies to pH values >5–6, when the rates of dissolution of smectites and zeolites are expected to be small (e.g. Chipera and Apps 2001; Rozalén et al. 2008). In such cases, the SSA_{BET}-normalised concentrations of dissolved elements are likely to be underestimated, and the use of SSA_{geo} for normalising concentrations seems more appropriate. For example, the seemingly low hydroxyl radical generation value (<0.5 μmol m^{-2}) reported for various *phase I* ash samples by Horwell et al. (2013) may be an artefact related to the use of SSA_{BET} to normalise the ash surface reactivity; replacing SSA_{BET} by SSA_{geo} in the estimates increases hydroxyl radical generation for *phase I* ash to levels above that found for *phase III* ash (i.e. sample EY-10-13 in Horwell et al.'s study).

Seifert et al. (2011) reported significant ice formation in clouds affected by transport of the Eyjafjallajökull ash over Europe. Similarly, Bingemer et al. (2011) emphasised the notable efficiency of the airborne ash to form ice nuclei. The presence of ice in volcanic plumes/clouds and ash-affected meteorological clouds impacts on their microphysical properties. The factors which determine the ability of ash to trigger ice formation remain poorly understood. Previous studies on mineral dust indicate that kaolinite and smectites play a key role in ice nucleation activities (e.g. Pinti et al. 2012 and references therein), although the importance of feldspar minerals for ice nucleation by mineral dust in mixed-phase clouds has

Fig. 3 X-ray diffractograms of the <0.2-μm size fraction of EYJ-A3 (*phase I*) ash subjected to K saturation (*K*) followed by heating at 105 °C (*K 105*), 300 °C (*K 300*) and 500 °C (*K 500*) and Mg saturation (*Mg*) followed by ethylene glycol solvatation (*Mg Eg*). The peaks corresponding to plagioclases (*Pl*) and smectites (*Sm*) are shown
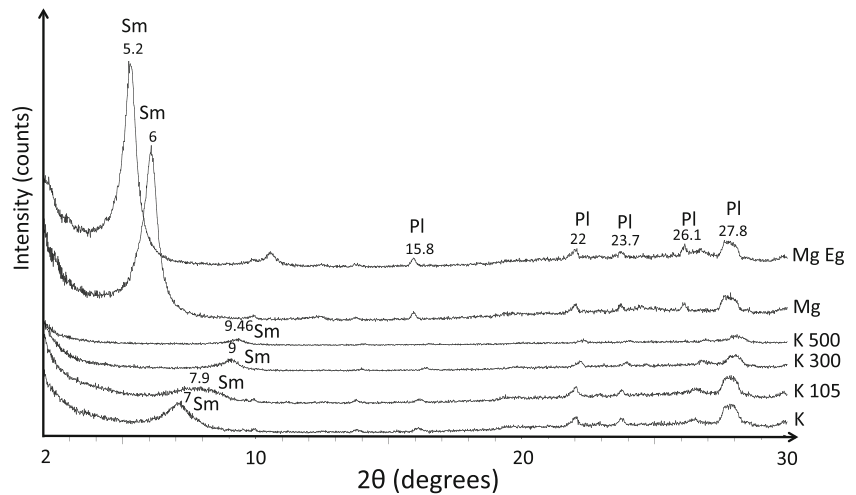

recently been put forward (Atkinson et al. 2013). It has also been shown that the highly microporous zeolite minerals are able to accommodate homogeneous freezing of capillary-held water, a pre-activation phenomenon that enhances the ice formation ability of an ice nucleating particle (Wagner et al. 2015). On this basis, we suggest that incorporation of smectites and zeolites in *phase I* ash may have influenced the ability of the airborne fraction to act as ice nuclei during transport in the atmosphere.

Several authors have highlighted that particle aggregation exerted a strong influence on ash dispersion and deposition during the 2010 eruption of Eyjafjallajökull volcano (Bonadonna et al. 2011; Taddeucci et al. 2011). The process driving aggregation in ash clouds is not yet fully elucidated but involves electrostatic attraction, van der Waals forces and liquid bonding (Brown et al. 2012). The availability of liquid

water is regarded as a key control on aggregation. Here we suggest that the presence of smectites in *phase I* ash also may have influenced its propensity to form aggregates as smectites are notorious aggregating agents in aqueous suspensions, owing to the development of a double-charge layer around the clay's platelet faces (Pusch and Yong 2006). Interestingly, Navrátil et al. (2013) mentioned the presence of aggregated hydrous aluminosilicates, tentatively identified as smectites, micas, chlorites and zeolites, in the Eyjafjallajökull ash material contained in dust samples collected in Prague, Czech Republic, between 15 April and 20 May 2010. This could be evidence for particle aggregation processes involving smectites during the long-range transport of the volcanic ash cloud.

The *phase I* ash fallout not only brought fresh silicate materials to the soil surface but also saponite and zeolites in non-

Fig. 4 X-ray diffractogram of the <0.2-μm size fraction of EYJ-A3 (*phase I*) ash. The *arrows* indicate the main peaks corresponding to plagioclase (*Pl*), pyroxenes (*Py*), smectites (*Sm*) and zeolites (*Z*)
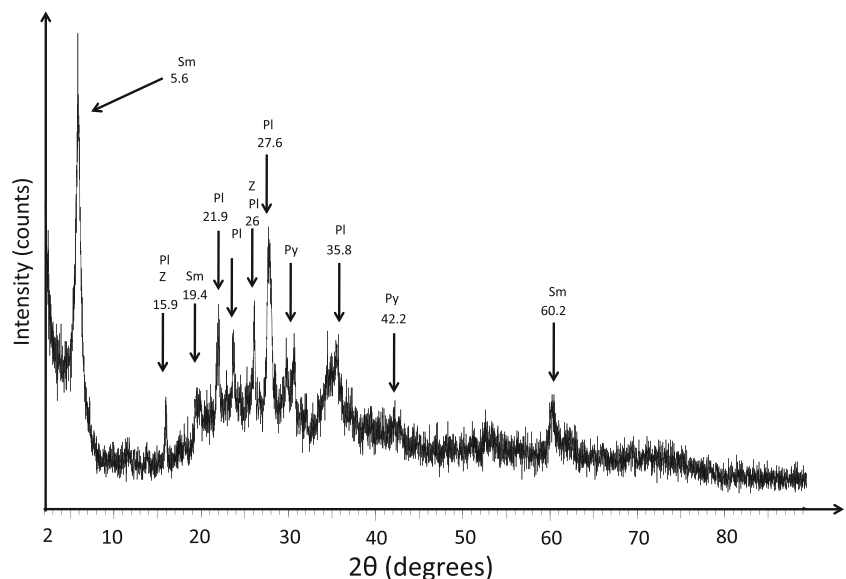
negligible quantities. All the soils affected by the Eyjafjallajökull eruption are volcanic soils (i.e. soils derived from volcanogenic materials; Arnalds 2004). The origin of layer silicate minerals of the 2:1 type such as smectites in volcanic soils has been long debated and various theories have been proposed, among them in situ formation due to weathering, eolian addition from distant sources or inheritance of hydrothermally altered materials in the volcanic parent material (Dahlgren et al. 2004 and references therein). Our results add further credence to the idea that, in active volcanic regions, these minerals can be sourced to ash deposition (e.g. Pevear et al. 1982; LaManna and Ugolini 1987; Jongmans et al. 1994). Based on the measured smectite content in the *phase I* ash (Table 2) and using isopach maps of ash distribution corresponding to *phase I* of the Eyjafjallajökull eruption (Gudmundsson et al. 2012), we roughly estimate that the total amount of smectites (mainly saponite) added to the soil between 14 and 18 April 2010 is ~1.2 kg m^{-2}. However, saponite is not stable in the soil weathering environment and is not expected to influence soil mineralogy durably (Meunier 2005).

Concluding remarks

Volcanic eruptions involving hydrothermally altered rocks produce ash with a mineralogy that may significantly depart from that commonly observed for ash from purely magmatic activity. The materials from the 2010 Eyjafjallajökull eruption, which transitioned from phreatomagmatic (*phase I*) to magmatic (*phases II* and *III*) within a few days, exemplify such mineralogical differences: smectites (mainly saponite) and zeolites occur in significant amounts in the *phase I* ash but are negligible in the *phase II* ash and absent in the *phase III* ash. The secondary minerals in *phase I* ash were probably eroded from pre-existing subglacial altered rocks, although a small proportion may have formed within the water/ice-filled vent through which ash was injected and recycled during the initial phase of the eruption. Further measurements of the oxygen isotopic composition of oxygen in smectites from *phase I* ash may shed light on the importance of the latter mechanism (e.g. Mizota and Faure 1998).

We show that the presence of smectites and zeolites considerably increases the specific surface area of the *phase I* ash, with repercussions for correctly assessing its surface reactivity, and thus its potential health hazard. While these minerals correspond to the ash's respirable-sized material, they do not seem to pose a significant health hazard. Nevertheless, additional mineralogical studies are recommended in order to fully dismiss occurrence of fibrous zeolites. Incorporation of smectites and zeolites in *phase I* ash may also have influenced its ability to act as ice nuclei. In addition, smectites may have enhanced the ash's aggregating properties. Finally, our results support previous claims that ash fallout is a plausible source of 2:1-type clay minerals in volcanic soils. Overall, we

emphasise the need for considering clay and zeolite minerals in ash from phreatic and phreatomagmatic eruptions as potentially important attributes for better understanding ash behaviour and fate in the environment. This may be particularly relevant in the context of global warming where subglacial eruptions involving altered rock masses may become more frequent in Iceland and elsewhere (Tuffen 2010).

References

Arnalds O (2004) Volcanic soils of Iceland. Catena 56:3–20

Atkinson JD, Murray BJ, Woodhouse MT, Whale TF, Baustian KJ, Carslaw KS, Dobbie S, O'Sullivan D, Malkin TL (2013) The importance of feldspar for ice nucleation by mineral dust in mixed-phase clouds. Nature 498:355–358

Baris I, Grandjean P (2006) Prospective study of mesothelioma mortality in Turkish villages with exposure to fibrous zeolite Y. J Natl Cancer I 98:414–417

Bingemer H, Klein H, Ebert M, Haunold W, Bundke U, Herrmann T, Kandler K, Müller-Ebert D, Weinbruch S, Judt A, Ardon-Dryer K, Levin Z, Curtius J (2011) Atmospheric ice nuclei in the Eyjafjallajökull volcanic ash plume. Atmos Chem Phys Discuss 11:2733–2748

Bish DL, Post JE (1993) Quantitative mineralogical analysis using the Rietveld full-pattern fitting method. Am Mineral 78:932–940

Björnsson H (2003) Subglacial lakes and jökulhlaups in Iceland. Glob Planet Chang 35:255–271

Bonadonna C, Genco R, Gouhier M, Pistolesi M, Cioni R, Alfano F, Hoskuldsson A, Ripepe M (2011) Tephra sedimentation during the 2010 Eyjafjallajökull eruption (Iceland) from deposit, radar, and satellite observations. J Geophys Res 116, B12202. doi:10.1029/2011JB008462

Brantley SL, Mellott NP (2000) Surface area and porosity of primary silicate minerals. Am Mineral 85:1767–1783

Brown RJ, Bonadonna C, Durant AJ (2012) A review of volcanic ash aggregation. Phys Chem Earth 45:65–78

Browne PRL (1978) Hydrothermal alteration in active geothermal fields. Annu Rev Earth Planet Sci 6:229–250

Cadiboche YM, Feller C, Larqué P, Sobesk O (1987) Sur un double mécanisme d'acidification des sols sous l'influence de cendres volcaniques récentes. Le cas de la Soufrière de Guadeloupe après les éruptions de 1976–1977. CR Acad Sci Paris 15:935–938

Chipera SJ, Apps JA (2001) Geochemical stability of natural zeolites. Rev Mineral Geochem 45:117–161

Cioni R, Pistolesi M, Bertagnini A, Bonadonna C, Hoskuldsson A, Scateni B (2014) Insights into the dynamics and evolution of the 2010 Eyjafjallajökull summit eruption (Iceland) provided by volcanic ash textures. Earth Planet Sci Lett 394:111–123

Cousins CR, Crawford IA, Carrivick JL, Gunn M, Harris J, Kee TP, Karlsson M, Carmody L, Cockell C, Herschy B, Joy KH (2013) Glaciovolcanic hydrothermal environments in Iceland and implications for their detection on Mars. J Volcanol Geotherm Res 256:61–77

Dahlgren RA, Saigusa M, Ugolini FC (2004) The nature, properties and management of volcanic soils. Adv Agron 82:113–182

Dellino P, Gudmundsson MT, Larsen G, Mele D, Stevenson JA, Thordarson T, Zimanowski B (2012) Ash from the Eyjafjallajökull eruption (Iceland): fragmentation processes and aerodynamic behavior. J Geophys Res 117:B00C04. doi:10.1029/2011JB008726

Delmelle P, Villiéras F, Pelletier M (2005) Surface area, porosity and water adsorption properties of fine volcanic ash particles. Bull Volcanol 67:160–169

Favier V, Coudrain A, Cadier E, Francou B, Ayabaca E, Maisincho L, Praderio E, Villacis M, Wagnon P (2008) Evidence of groundwater flow on Antisana ice-covered volcano, Ecuador. Hydrol Sci J 53:278–291

Fejdi P, Holocsy A (2001) Relationship between crystal morphology and preferred orientation in polycrystalline specimens for diffraction experiments. Mater Struct 8:22–24

Garchar L, Wendlandt R, Martini B, Owens L (2012) Geochemistry of a sub-glacial volcanic hydrothermal system at Mount Spurr, Alaska. Proceedings, Thirty-Seventh Workshop on Geothermal Reservoir Engineering, Stanford University, Stanford, California, SGP-TR-194

Gislason SR, Hassenkam T, Nedel S, Bovet N, Eiriksdottir ES, Alfredsson HA, Hem CP, Balogh ZI, Dideriksen K, Oskarsson N, Sigfusson B, Larsen G, Stipp SLS (2011) Characterization of Eyjafjallajökull volcanic ash particles and a protocol for rapid risk assessment. Proc Natl Acad Sci 108:7307–7312

Gudmundsson MT, Thordarson T, Hoskuldsson A, Larsen G, Bjornsson H, Prata FJ, Oddsson B, Magnusson E, Hognadottir T, Petersen GN, Hayward CL, Stevenson JA, Jonsdottir I (2012) Ash generation and distribution from the April-May 2010 eruption of Eyjafjallajökull, Iceland. Nat Sci Rep 2:572–594

Horwell CJ, Baxter PJ (2006) The respiratory health hazards of volcanic ash: a review for volcanic risk mitigation. Bull Volcanol 69(1):1–24

Horwell CJ, Baxter PJ, Hillman SE, Calkins JA, Damby DE, Delmelle P, Donaldson K, Dunster C, Fubini B, Kelly FJ, Le Blond JS, Livi KJT, Murphy F, Nattrass C, Sweeney S, Tetley TD, Thordarson T, Tomatis M (2013) Physicochemical and toxicological profiling of ash from the 2010 and 2011 eruptions of Eyjafjallajökull and Grímsvötn volcanoes, Iceland, using a rapid respiratory hazard assessment protocol. Environ Res J 127:63–73

International Agency for Research on Cancer (2012) IARC monographs on the evaluation of carcinogenic risks to humans: arsenic, metals, fibres and dusts. Volume 100C. A review of humans carcinogens. http://monographs.iarc.fr/ENG/Monographs/vol100C/mono100C-1.pdf. Accessed 4 Jan 2016

International Centre for Diffraction Data (2013) Be confident with pdf2. http://www.icdd.com/products/technicalbulletins/PDF-2_Technical_%20Bulletin.pdf. Accessed 5 Aug 2015

Jongmans AG, Van Oort F, Nieuwenhuyse A, Buurman P, Jaunet AM, Van Doesburg JDJ (1994) Inheritance of 2:1 phyllosilicates in Costa Rican andisols. SSSAJ 58:494–501

Kanno I, Honjo Y, Kuwano Y (1961) Clay minerals of volcanic ash erupted from the Shinmoe-dake of the Kirishima volcanic cluster on February 17, 1959. Appl Clay Sci 3:214–224 (in Japanese)

Kodama H (2012) Phyllosilicates. In: Huang PM, Li Y, Summer ME (eds) Handbook of soil science, properties and processes. CRC, New York, pp 1–72

Kondo Y, Kondo R, Katsui Y (1978) Clay minerals of the volcanic ash erupted from the volcano Usu in August, 1977. J Sci Soil Manure 49:167–169 (in Japanese)

Kristjansson L, Johannesson H, Eiriksson J, Gudmudsson AI (1988) Brunhes-Matuyama paleomagnetism in three lava sections in Iceland. Can J Earth Sci 25:215–225

Lamanna JM, Ugolini FC (1987) Trioctahedral vermiculite in a 1980 pyroclastic flow, Mt. St. Helens, Washington. J Soil Sci 143:162–167

Loughlin SC (1995) The evolution of the Eyjafjoll volcanic system, southern Iceland. Durham University. Available at Durham E-Theses Online, Durhamntheses, http://etheses.dur.ac.uk/1456/. Accessed 1 Oct 2015

Loughlin SC (2002) Facies analysis of proximal subglacial and proglacial volcaniclastic successions at the Eyjafjallajökull central volcano, southern Iceland. Geol Soc Spec Publ 202:149–178

Magnússon E, Gudmundsson MT, Roberts MJ, Sigurðsson G, Höskuldsson F, Oddsson B (2012) Ice-volcano interactions during the 2010 Eyjafjallajökull eruption, as revealed by airborne imaging radar. J Geophys Res 117, B07405. doi:10.1029/2012JB009250

Mertens G, Snellings R, Van Balen K, Bicer-Simsir B, Verlooy P, Elsen J (2009) Pozzolanic reactions of common natural zeolites with lime and parameters affecting their reactivity. Cem Concr Res 39:233–240

Meunier A (2005) Clays. Springer, Berlin

Mizota C, Faure K (1998) Hydrothermal origin of smectite in volcanic ash. Clay Clay Miner 46:178–182

Navrátil T, Hladil J, Strnad L, Koptíková L, Skála R (2013) Volcanic ash particulate matter from the 2010 Eyjafjallajökull eruption in dust deposition at Prague, central Europe. Aeolian Res 9:191–202

Nogami K, Hirabayashi JI, Ohba T, Yoshiike Y (2000) The 1997 phreatic eruption of Akita-Yakeyama volcano, northeast Japan: insight into the hydrothermal processes. Earth Planets Space 52:229–236

Ohba T, Kitade Y (2005) Subvolcanic hydrothermal systems: implications from hydrothermal minerals in hydrovolcanic ash. J Volcanol Geotherm Res 145:249–262

Ohba T, Nakagawa M (2002) Minerals in volcanic ash 2: non-magmatic minerals. Glob Environ Res 6:53–59

Pansu M, Gautheyrou J (2006) Handbook of soil analysis: mineralogical, organic and inorganic methods. Springer, Berlin, 993 p

Pevear DR, Dethier DP, Frank D (1982) Clay minerals in the 1980 deposits from Mount St. Helens. Clay Clay Miner 30:241–252

Pinti V, Marcolli C, Zobrist B, Hoyle CR, Peter T (2012) Ice nucleation efficiency of clay minerals in the immersion mode. Atmos Chem Phys 12:5859–5878

Pusch R, Yong RN (2006) Microstructure of smectite, clays and engineering performance. Taylor and Francis, London, 328p

Rietveld HM (1969) A profile refinement method for nuclear and magnetic structures. J Appl Crystallogr 2:65–71

Riley CM, Rose WI, Bluth GJS (2003) Quantitative shape measurements of distal volcanic ash. J Geophys Res 108(B10):2504. doi:10.1029/2001JB000818

Rom WN, Casey KR, Parry WT, Mjaatvedt CH, Moatamed F (1983) Health implications of natural fibrous zeolites for the Intermountain West. Environ Res J 30:1–8

Rozalén ML, Huertas FJ, Brady PV, Cama J, García-Palma S, Linares J (2008) Experimental study of the effect of pH on the kinetics of montmorillonite dissolution at 25 °C. Geochim Cosmochim Acta 72:4224–4253

Seifert P, Ansmann A, Gross S, Freudenthaler V, Heinold B, Hiebsch A, Mattis I, Schmidt J, Schnell F, Tesche M, Wandinger U, Wiegner M (2011) Ice formation in ash influenced clouds after the eruption of the Eyjafjallajökull volcano in April 2010. J Geophys Res 116: D00U04. doi:10.1029/2011JD015702

Sigmarsson O, Vlastelic I, Andreasen R, Bindeman I, Devidal JL, Moune S, Keiding JK, Larsen G, Höskuldsson G, Thordarson T (2011) Remobilization of silicic intrusion by mafic magmas during the 2010 Eyjafjallajökull eruption. Solid Earth 2:271–281

Stroncik N, Schmincke HU (2002) Palagonite—a review. Int J Earth Sci (Geol Rundsch) 91:680–697

Taddeucci J, Scarlato P, Montanaro C, Cimarelli C, Del Bello E, Freda C, Andronico D, Gudmundsson MT, Dingwell DB (2011) Aggregation-dominated ash settling from the Eyjafjallajökull volcanic cloud illuminated by field and laboratory high-speed imaging. Geology 39:891–894

Taylor JC, Matulis CE (1991) Absorption contrast effects in the quantitative XRD analysis of powders by full multiphase profile refinement. J Appl Crystallogr 24:14–17

Tuffen H (2010) How will melting of ice affect volcanic hazards in the twenty-first century? Phil Trans R Soc A 368:2535–2558

Utada M (2001) Zeolites in hydrothermally altered rocks. Rev Mineral Geochem 45:305–322

Wagner R, Kiselev A, Möhler O, Saathoff H, Steinke I (2015) Pre-activation of ice nucleating particles by the pore condensation and freezing mechanism. Atmos Chem Phys Discuss 15:28999–29046

Ward CR, French D (2006) Determination of glass content and estimation of glass composition in fly ash using quantitative X-ray diffractometry. Fuel 85:2268–2277

Warner NH, Farmer JD (2010) Subglacial hydrothermal alteration minerals in jökulhlaup deposits of southern Iceland, with implications for detecting past or present habitable environments on Mars. Astrobiology 10:523–547

Winburn RS, Grier DG, McCarthy GJ, Peterson RB (2000) Rietveld quantitative X-ray diffraction analysis of NIST fly ash standard reference materials. Powder Diffract 15:163–172

World Health Organization (2005) Bentonite, kaolin and selected clay minerals. Environmental Health Criteria 231, 175p. https://www.who.int/ipcs/publications/ehc/ehc_231.pdf. Accessed 4 Jan 2016